MATHEMATICAL APPROACH TO ESTIMATION OF THE STABILIZING EFFECT OF GEOSYNTHETIC FLOATS FOR THE STABILITY OF HANDS

МАТЕМАТИЧНИЙ ПІДХІД ДО ОЦІНКИ СТАБІЛІЗУЮЧОГО ЕФЕКТУ ГЕОСИНТЕТИЧНИХ ПРОШАРКІВ ДЛЯ СТІЙКОСТІ УКОСІВ

Dahoua Lamri, 19 City Mohamed Benbeguag, Sétif,19000, Algéria.

https://orcid.org/0000-0002-9007-9394

Savenko Viacheslav Y., Doctor of Technical Sciences, Professor, National Transport University, Head of Department, Department of Transport Construction and Property Management

http://orcid.org/0000-0001-8174-7728

Riheb Hadji, PhD. Department of Earth Sciences, Ferhat Abbas University of Setif

http://orcid.org/0000-0002-9632-0812

Abstract: The change of the boundary conditions is the main responsible for the slopes equilibrium disturbance, and mass wasting. Under normal climatic conditions, unconsolidated dry grains remain stable for a given internal friction angle. This angle increases if the soil is slightly moistened, since the surface tension between the water and the soil particles tends to fix the grains. During intense precipitation or snow clearing, water infiltration causes a reduction in the values of the friction angle (φ') and the cohesion (c') of the grains, which threatens the stability of the slope, this latter is accentuated by vibrations, where liquefaction of the soil occurs. Supported by the decline of the resistance to inter granular friction, the fall of the mechanical characteristics of the soil will lead to the translation of the Mohr circle towards a rupture envelope curve. The incorporation of geotextile sheets can improve the stability of road embankments. This exerts stabilizing forces opposing the forces disturbing the slope equilibrium. These forces are not taken into account by the Bishop method, which is based on a good number of software such as Geostudio / slope. Our work consists in developing a mathematical approach to: introducing variable values of (c') and (φ') into the rupture criterion to take into account water infiltration, introducing a new parameter (F s) to take account of the effect of the seismic stresses, introducing a force (r) to take account of the infiltrated water portion. Finally, stabilizing forces generated by the introduction of géosynthetic sheets (Geo) are engaged in the polygon of the Bishop forces. The result shows that the action of water is the main disruptive force of the slope and the action of the geotextiles is the main stabilizing force.

Key words: internal friction angle, cohesion, geosynthetics, slope stability, Bishop's method.

Problem statement: Shifts in the soil among geodynamic phenomena are the most common and most serious on the surface of the earth. They cause a natural and continuous change in the relief and occur, as a rule, either unexpectedly, especially during earthquakes, and / or during intense periods of rains with prolonged precipitation and the combined action of geological factors of different geomorphology. The state of the problem in the field of equilibrium of the slopes is quite developed in the world [1, 2, 3] and a little less in Algeria [4, 5]. There is a distinction between structural instability and geotechnical. The first form occurs in arrays at low voltages in well-developed geological structures. They are induced from geological breaks arising from the effect of their own weight of materials as a result of seismic actions or human activity [6]. The second kind arises due to excessive stresses in the soil massif [7, 8]. Methods for studying the instability of rocks are also empirical in classification [9] (Bieniawski, 1993). Methods of calculating the stability of slopes: analytical [10, 11]; digital [12] and, more recently, geomechanical [13]. For soils, methods are based on the calculation of limiting equilibrium (Bishop, Felenius, Yambo, Morgenstern-Price, Spencerai et al.) Are the most commonly used [14]. Comparison of the safety coefficients of different methods for calculating the stability of the slopes advances the Bishop method as the most favorable for the use of the mathematical approach (Figure 1) when calculating the safety coefficient for a natural slope, subject to destructive effects, the presence of groundwater and stabilization by introducing geotextile layers.

In accordance with the simplified and strict Bishop method, effective stresses depend on the water level in the soil, which also corresponds to the Terzagi assumption: $\sigma' = \sigma - u$ (without compaction) [14].

What is not obvious, since the pore pressure may increase due to overload caused by suction during draining of the soil; The principle of Terzagi was changed by Bishop, who obtained the equation:

$$(\sigma' = \sigma - Ua + \chi.(Ua - Uw)); \quad (1)$$

where χ- is the coefficient depending on the shear forces or consolidation, and σ, Ua and Uw, respectively, are the general stress tensor, air pressure and water pressure, and S = (Ua-Uw) is absorption [15] (Figure 1). Tensores of stress are expressed in the form of vectors of six components. In our approach, the soil particles and the liquid are incompressible, and the air pressure is assumed to be the same as atmospheric pressure: Ua = Pt.

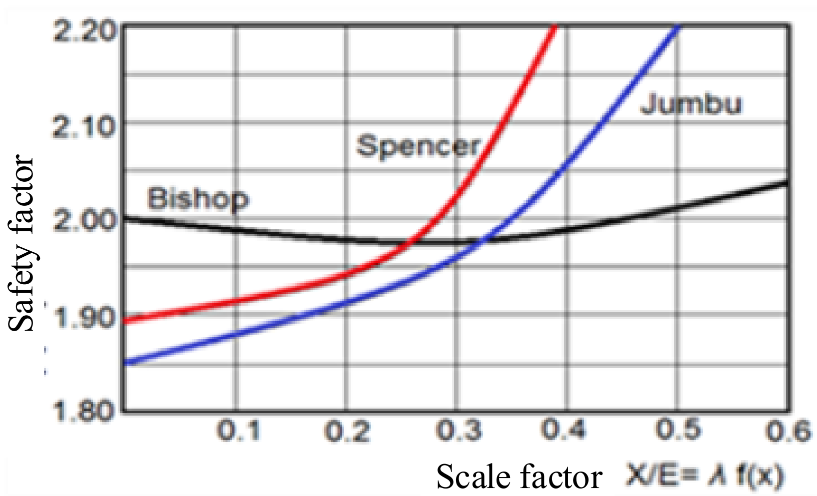

Figure 1 – Comparison of the safety coefficients of the three methods of limiting equilibrium.
Рисунок 1 – Порівняння коефіцієнтів безпеки трьох методів обмеження рівноваги.

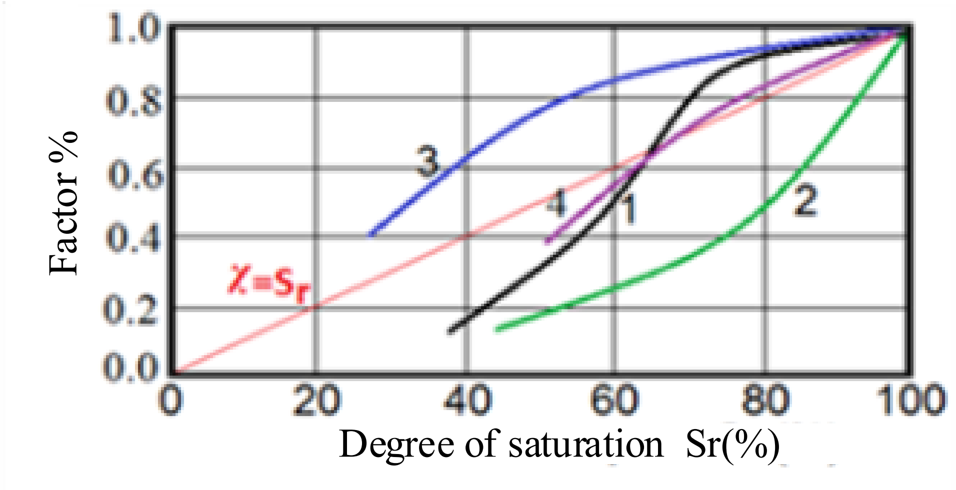

Figure 2 – Development of the coefficient χ depending on the degree of saturation:
1: Sealed clay; 2: Dusty loam; 3: Light loam; 4: White clay
At the first stage, this assumption will be used in our approach.

Рисунок 2 – Розробка коефіцієнта χ в залежності від ступеня насичення:
1: Герметична глина; 2: Пильний суглинок; 3: Легкий суглинок; 4: Біла глина
На першому етапі це припущення буде використано в нашому підході.

2. Methodology: The method consists in introducing the values of the variables (c ') and (φ') into the break criterion of the Mora-Coulomb law, the new parameter (Fs) for mapping the influence of seismic loads, the force (r) in the polygon of the Bishop forces for displaying the proportion of infiltration water and force (Geo) generated by the introduction of geosynthetic layers.

A- Influence of groundwater availability: Cyclical change in pore pressure, causes a significant reduction in the interaction forces in the soil, which can lead to a significant disturbance of the stressed state in the slope, even causing irreversible deformations. After a flood, melting snow, etc. a significant amount of infiltration water already seeping into the ground, as a rule, will be released from the slope by using the flow force of the next hyperbolic trajectory (related to the permeability of the medium) (Figure 3). This phenomenon was studied in the work of RICHARDS [16], its equation:

$$\mathrm{Div}\ (k(p)\overrightarrow{\mathrm{grad}}(\varphi))=c\frac{\partial\varphi}{\partial t} \qquad (2)$$

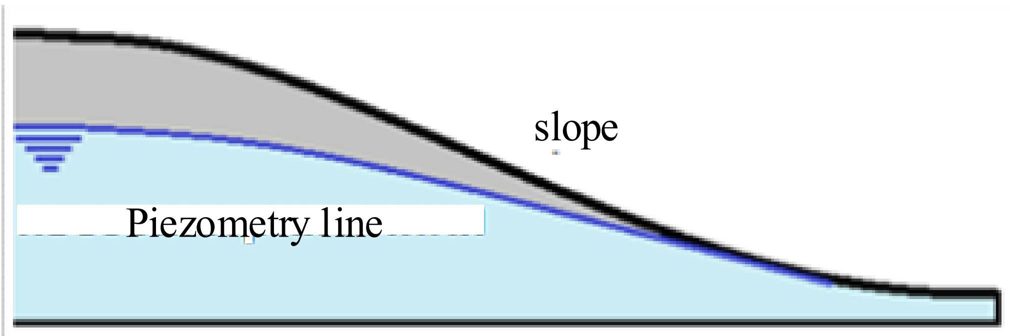

Figure 3 – The flow of groundwater in accordance with the Richards equation
Рисунок 3 – Потік грунтових вод відповідно до рівняння Річардса

On the basis of the general theory of aquifers, the RICHARDS equation [16] and the DEPUIT equation [16] have two forces: the first arises from the groundwater pore pressure, the second is caused by the flow of seepage water (it can be decisive in provoking slip, especially if the flow direction coincides with the slope slope) [17]. However, do not neglect the decrease in shear resistance caused by the action of water along the sliding surface (Figure 4):

$$ra= \frac{\Delta M_{é}}{\Delta M_p} = \frac{\gamma_w}{\gamma} \cdot \frac{\sin\alpha \sin(\theta+\alpha)}{\cos\theta} \quad (3)$$

where: Mé is the shearing moment due to the strength of the flow, and Mp is the shear moment due to the weight.

According to the data of [18], this equation takes into account the action of the water flow in comparison with the intrinsic weight of the soil layer. The latter corresponds to certain values of α, and θ, (30 °, 60 °, respectively). The component $\frac{\gamma_w}{\gamma}$, is significant, especially when the values of γ and γw are close in value. FIILIAT [19] proposed the law of the distribution of the water flow on the slope (this method gives the most satisfactory results and has less criticism of the researchers), which connects the shear forces, the normal effective stress and the shearing stress:

$$\sigma=\Sigma\gamma_i.\hbar._i\cos^2\alpha(\lambda+\mu.\tan\alpha), \quad (4)$$

where λ- is a compressibility.

Some methods for calculating the circular cylindrical slip surface make extensive use of this equation [20], in our approach we introduce the force of the water flow (r) directly into the Bishop's polygon diagram.

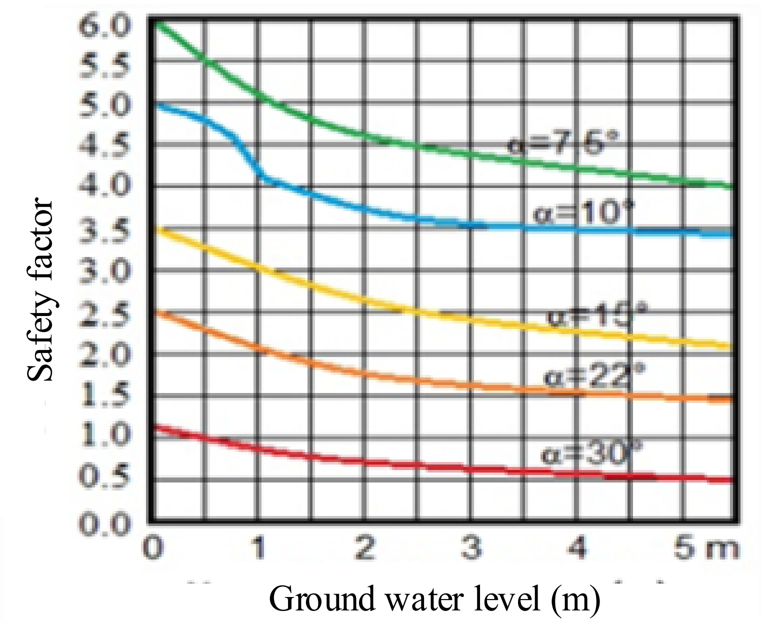

Figure 4 – The change in the safety factor (with different angles of inclination α) depending on the water table.

Рисунок 4 – Зміна коефіцієнта безпеки (з різними кутами нахилу α) залежно від стоку води.

B- Influence of seismic loading: Flowability is a direct result of seismic vibrations on the location of grains in the ground, these impacts are very harmful for stability. If the grain size curve of the soil sample is found in the category of medium and fine sand, with a uniformity coefficient Cu = <2, then there are large risks of destruction. The potential for fluidity is defined in [21] as the ability of the soil to reach the limiting state under a seismic load. It depends on the type and initial state of the soil compaction (Figure 5).

$$CSR_{7.5} = \frac{\tau}{\sigma'_{vo}}, \quad (5)$$

where CSR7.5 is the ratio of cyclic stresses for the magnitude of the earthquake readout M = 7.5 on the Richter scale:

$$CRR_{7.5} = 0.833 / (q.c_{iN}).0.001+0.05 \quad (6)$$

$$F = CRR_{7.5} / CSR_{7.5} \quad (7)$$

where CRR7.5 - stresses to fluidity (for an earthquake of magnitude M = 7.5 on the Richter scale.

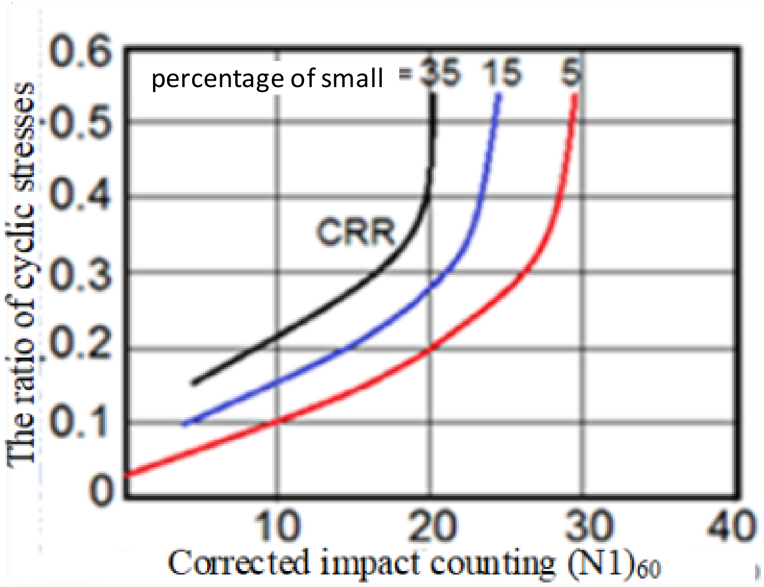

Figure 5 – Curves CSR7.5, depending on SPT and percentage of fine particles [20]
Рисунок 5 – Криві CSR7.5, залежно від SPT та відсотка дрібних частинок [20]

This indicator gives the ratio of the shear stress τ caused by seismic loads and effective geostatic stress (σ'v), depending on the penetration resistance SPT of ISO 22476-3, ASTM D1586 [22].

At the bottom of the slope, the shear stress due to the earthquake is determined by the peak earthquake acceleration (ah) (Swiss standards), and with the SEED reduction factor (rd) [21].

$$\tau = 0.6\ 5\ .\frac{a_h}{g}.\sigma_v.r_d \tag{8}$$

In the body of the slope it is expressed in terms of the maximum acceleration (ag) of the active center of gravity of the layer [23].

$$\tau = 0.65\ .\ \frac{a_g}{g}.\ \sigma_v \tag{9}$$

The maximum accelerations (amax) are determined by the sum of the spectral values of the acceleration (ai), each spectrum of their reaction (ωi) is corrected by the velocity of the effect (vs) [24].

$$a_{max} = [(1.60xa_1)^2 + (1.06xa_2)^2 + (0.86xa_3)^2]^{0.5} \tag{10}$$

$$\omega_i = c^{st}\frac{v_s}{h}\ P = \frac{2\pi}{\omega} \tag{11}$$

To replace the stresses by the acting forces:

- The horizontal force is the product of the average acceleration per block mass:

$$F_{horizontale} = a_{moy}\ .\ m \tag{12}$$

- The vertical force connects the vertical component of the seismic acceleration to the block mass:

$$F_{verticale} = a_{vert}\ .m \leftrightarrow\ F_{verticale} = 0.66\ a_{horizontale}\ .m \tag{13}$$

These two forces are used to use the mathematical approach in [25, 26].

C - Influence of water content on shallow grounds: The phenomenon of bond failure in undrained soils of undisturbed structure, and residual adhesion in finely dispersed saturated soils, was investigated using a shear device for measuring adhesion for water content variables (Table 1).

Table 1 – Changing the adhesion depending on the water content (measured by the Micro-Harvard)
Таблиця 1 – Зміна адгезії залежно від вмісту води (вимірюється мікро-Гарвардом)

Water content %	20	22	25	35	40	50	60
Cohesion in the soil of an undisturbed structure (kPa)	0.38	2.07	4.65	3.81	3.47	3.35	0.09
Residual grip (kPa)	0.19	0.77	1.33	1.30	1.28	1.20	0.09

The increase in adhesion, depending on the increase in water content, is observed with an upward curved threshold corresponding to 25% of humidity, then decreases to very dangerous values beyond 55% of humidity. The shape of this curve varies depending on the lithological composition of the soil [27, 28].

We can introduce this component directly into the Bishop breakdown criterion. The same observation applies to the change in the angle of internal friction (hence, in the Bishop method, we use the coefficient (Kφ = 0.8) and (φ '= φ .Kφ.) Proceeding from this we obtain:

$$S = 1 / F\ (c'\ (w)\ \ell + N' \tan\varphi'\ (w). \quad (14)$$

D- Density analysis: Vulnerability of fine fractions to easy laying or washing out, affects the relative density of the soil, and varies with time, sometimes the density increases with compaction or consolidation, or decreases as a result of leaching or dissolving of fine fractions of the soil.

$$Dr = \frac{\gamma d - \gamma dmin}{\gamma dmax - \gamma dmin} \times \frac{\gamma dmax}{\gamma d} \quad (15)$$

We can introduce the term relative density directly in terms of mass:

$$(W = Dr.h.b.1). \quad (16)$$

E-Geotextile interlayers: The introduction of geosynthetics (schematically as a line in the 2D section) can significantly improve the equilibrium state of the slope. With this layer position, only the tangential component (GéoX) plays a role in equilibrium. The flexible characteristics of the interlayer do not affect the nanormal component (under compression) .

3. The mathematical approach

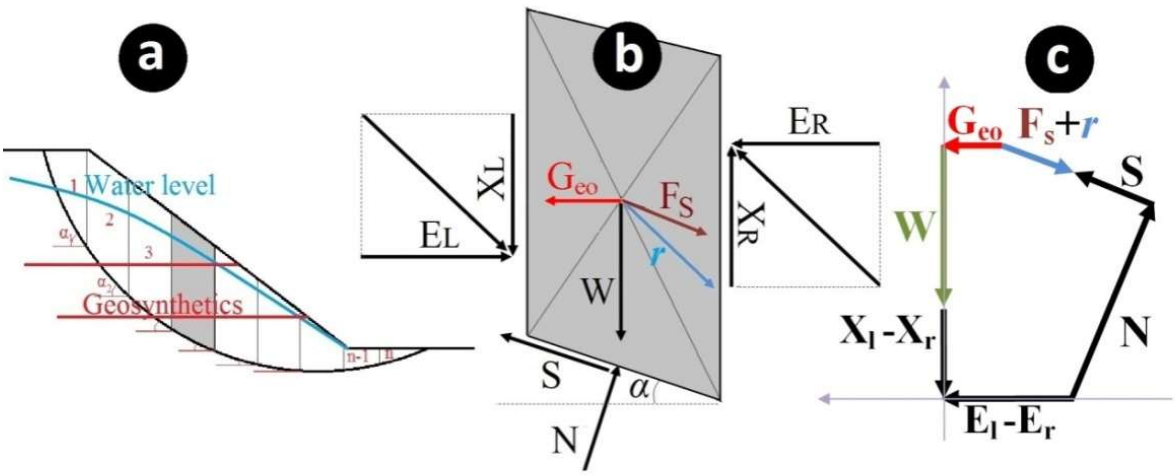

Figure 6 – a - Separation of the slope into blocks; b- Conditions of equilibrium; c is the Bishop's polygon.
Рисунок 6 – а - Поділ схилу на блоки; б - умови рівноваги; с - полігон єпископа.

Xl, XR, EL, ER - vertical and horizontal forces between blocks; W is its own weight;

S is the normal force; Geo - tensile forces in geotextiles, F - seismic forces;

r is the force associated with the flow of groundwater; α is the angle of the base segment; θ is the angle between the line of the piezometric level and the horizontal.

The Coulomb-Mora law:

$$S = \frac{1}{F}(c'(w)\,\ell + N.\tan\varphi'(w)) \tag{17}$$

The projection of forces on the vertical in the center of the section.

$$(N + u_a.\ell - \chi.\ell.s_e).\cos\alpha = W + (X_L - X_R) - S.\sin\alpha + (F^s_{vert} + r.\sin\theta) \tag{18}$$

the replacement of S according to (17):

$$(N + u_a.\ell - \chi.\ell.s_e)\cos\alpha = W + (x_l - x_r) - /F(c'(w)\,\ell + N.\tan\varphi'(w)).\ \sin\alpha + (F^s_{vert} + r.\sin\theta) \tag{19}$$

$$(N.\cos\alpha) + (u_a.\ell - \chi.\ell.s_e).\cos\alpha = W + (x_L - x_R) - (c'(w)\ell/F).\sin\alpha - N.\tan\varphi'(w).\sin\alpha/F) + (F^s_{vert} + r.\sin\theta) \tag{20}$$

where: c '(w), φ' (w): are residual characteristics due to material fatigue (see section C):

$$N.(\cos\alpha + (\tan\varphi'(w).\sin\alpha)/F) = W + (x_L - x_R) - \ell.\ (u_a - \chi.s_e).\cos\alpha - (c'(w)\sin\alpha/F) + (F^s_{vert} + r.\sin\theta). \tag{21}$$

$$N = \frac{\left(W + (x_L - x_R) - \ell.(u_a - \chi.s_e).\cos\alpha - \left(c'(w)\sin\alpha/_F\right) + (Fs_{vert} + r\sin\theta)\right)}{(\cos\alpha + (\tan\varphi'(w)\sin\alpha)/F)} \tag{22}$$

For clarity and simplicity, Bishop's method allowed to neglect the forces in the intermediate sections (which is present with a small difference between the blocks) and the center of gravity of the compartment is located at half its height. Moments with respect to the center of rotation of the sliding surface:

$$W.R_x = S.R - F^s_{vert}R_x - F^s_{horiz}(R.(\cos\alpha) - h/2) - r.\sin\theta.R_x - r.\cos\theta.(R.(\cos\alpha) - h/2) + G_{eo}(R.(\cos\alpha) - h/2) \tag{23}$$

$$W.R\sin\alpha = R.\tau\ell - F^s_{vert}R.\sin\alpha - F^s_{horiz}(R.(\cos\alpha) - h/2) - ((r\sin\theta.R\sin\alpha) + ((r\cos\theta - G_{eo}).(R(\cos\alpha) - h/2))) \tag{24}$$

When the destruction criterion (τ = c '+ σ.tanφ') is introduced into equation (24):

$$W.\ R\sin\alpha = R/F.\ [(c'(w)\ell + N\tan\varphi'(w)\ell) - (\ell\tan\varphi'(w).(u_a - \chi.s_e))] - [(F^s_{vert} + r\sin\theta)(R\sin\alpha)] - (F^s_{horiz} + r\cos\theta - G_{eo}).(R.(\cos\alpha) - h/2)] \tag{25}$$

$$F = \frac{R\,[(c'(w)\ell + N.\tan\varphi'(w)\ell) - (\ell\tan\varphi'(w).(ua - \chi.se))]}{WR\sin\alpha + [(Fsvert + r\sin\theta)(R\sin\alpha)] + [(Fs_{horiz} + r\cos\theta - Geo)\ (R.(\cos\alpha) - h/2)]} \tag{26}$$

$$F = \frac{[c'(w)\ell + N\tan\ \ '(w)] - [\ell\tan\varphi'(w).(ua - \chi.se)]}{WR\sin\ \ [(Fs_{vert} + r\sin\theta)(R\sin\alpha)] + [(Fs_{horiz} + r\cos\theta - G_{eo})\ (R.(\cos\alpha) - h/2)]}. \tag{27}$$

Substituting the values of N from (21) into (25) and taking into account the sum of the blocks:

$$F = \frac{\Sigma\,[[c'(w)\ell + \frac{\tan\varphi'(w)[W - (\ell\cos\alpha\ (ua - \chi.se))] + (c'(w)\sin\alpha/F) + Fsvert + r\sin\theta]}{\cos\alpha + (\tan\varphi'(w)\sin\alpha/F)} - \ell\,(ua - \chi.se)]}{\Sigma[W_i\sin\alpha_i + [(Fs_{horiz} + r_i\cos\theta_i - G_{eo})\left(co\ \ _i - \frac{h_i}{2R}\right)] + (r_i\sin\theta_i + \Sigma Fs_{vert})(\sin\alpha_i)]} \tag{28}$$

Replacing:

$$\frac{1}{m\propto} = \frac{(\sec\alpha)}{\frac{(1 + (\tan\varphi'(w).ta\ \ \ )}{F}} \tag{29}$$

We get:

$$F = \frac{c'(w)\ell + N\tan\ \ '(w)[W - (\ell co\ \ \ (ua - \chi.se))] + \left(c'\frac{(w)\sin\alpha}{F}\right) + Fs_{vert} + r\sin\theta\ ][1/m_\alpha] - \ell(ua - \chi.se)]}{\Sigma[W_i\sin\alpha_i + [(Fs_{horiz} + r_i\cos\theta_i - G_{eo})\ (\cos\alpha_i - h_i/2R)) + (r_i\sin\theta_i + \Sigma Fs_{vert})(\sin\alpha_i)]} \tag{30}$$

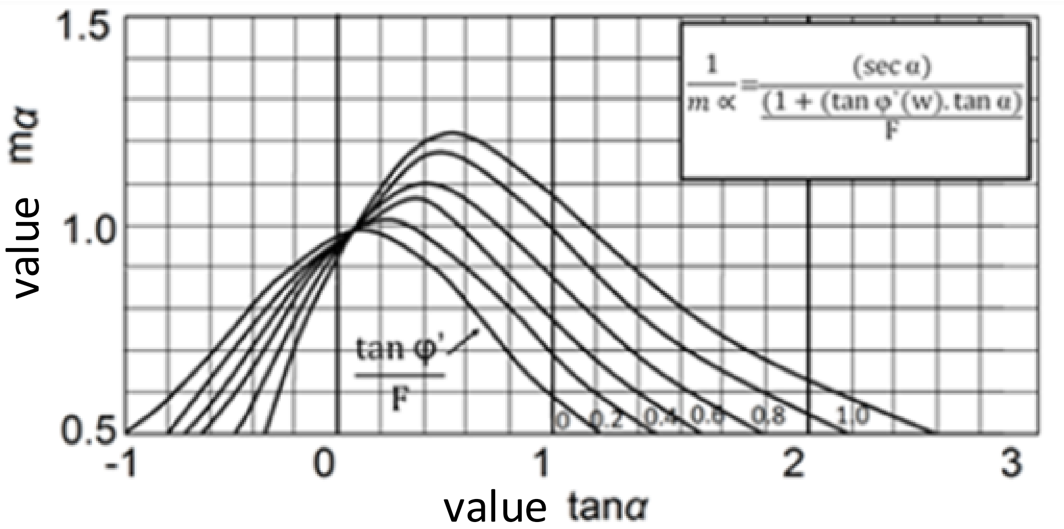

Figure 7 – Changing mα depending on tanφ '.
Рисунок 7 – Зміна mα залежно від tanφ '.

4. Results: Equation (30) is the result of a mathematical approach for the Bishop method. The appearance of seismic forces and due to the flow of water simultaneously with the numerator and in the denominator and the stretching force in the geotextile with a negative sign in the denominator (plays a positive role for stability) makes it possible to obtain the safety factor of the modified method and the simplified and exact Bishop method.

$$\text{At: } \varphi' = \varphi.K_{\varphi}; \text{ и } ru = \frac{u}{\text{Total vertical stress}} \quad (31)$$

$$\text{- simplified method: } F = \frac{\Sigma\{c'b + \tan\ '(W(1-ru))\}1/m\alpha}{\Sigma W \sin}; \quad (32)$$

$$\text{- exact method: } F = \frac{\Sigma\left\{\left(c'b + \tan\ '(W(1-ru))\right) + (xl - x\ )\right\}1/m\alpha}{\Sigma W \sin} \quad (33)$$

This allows us to obtain a safety interval in the design of the embankments and take into account the various forces affecting the equilibrium of the natural slope [29, 30].

5. Conclusions: The phenomenon of instability of road slopes under the influence of various external factors is not fully understood. Previous studies have shown that the level of groundwater in the slope had a large role in development during the movement of a natural or constructed slope [31]. In this article, the influence of various external factors on the stability of slopes was assessed. Using the Bishop method, we were able to establish a change in the safety factor, depending on the presence of geosynthetic layers, the availability of groundwater and seismic forces. Instability thus appears in connection with the behavior of the last two factors. The laying of geotextile layers plays a decisive role in the stabilization of slopes. The appearance of a retaining force from geotextiles in the denominator of the modified Bishop equation with a negative sign proves the strengthening of the structure due to the tension effect in the layers of geotextile.

With the use of software, this approach can be used to take these factors into account in limiting equilibrium calculations.

References

1. Varnes, D.J., Int. Association of Engineering Geology Commission on Landslides, 1984.
2. Frayssines, M. (2005). Contribution à l'évaluation de l'aléa éboulement rocheux (rupture) (Doctoral dissertation, Université Joseph-Fourier-Grenoble I).
3. Antoine, P., & Giraud, A. (1995). Typologie des mouvements de versants dans un contexte opérationnel. Bulletin of Engineering Geology and the Environment, 51(1), 57-62.

4. Guadri L, Hadji R, Zahri F, Raïs K (2015). The quarries edges stability in opencast mines: A case study of the Jebel Onk phosphate mine, NE Algeria. Arabian Journal of Geosciences Arab J Geosci 8:8987–8997.

5. Hadji R, Raïs K, Gadri L, Chouabi A, Hamed Y (2017) Slope failures characteristics and slope movement susceptibility assessment using GIS in a medium scale: a case study from Ouled Driss and Machroha municipalities, Northeastern of Algeria, Arabian Journal for Science and Engineering, Arab J SciEng 42:281–300.

6. Malatrait N., 1975. Analyse et classement des mouvements gravitaires, Feuille St. Jean-de-Maurienne. Thèse d'état, Université Joseph Fourier, Grenoble I.

7. Hoek E., Brown E.T., 1980. Empirical strength criterion for rock masses. Journal of the Geotechnical engineering Division, ASCE, Vol. 106, n° GT9, 1980, 1013-1035.

8. Hoek E., 1990. Practical Rock Engineering 3-Slope Stability and Rockfalls, Chapter 9.

9. Bieniawski Z.T. Engineering Rock Mass Classifications.J. Wiley, New York, 1989.

10. Goodman, R. E., & Shi, G. H. (1985). Block theory and its application to rock engineering (p. 338). Englewood Cliffs, NJ: Prentice-Hall.

11. Vengeon, J. M. (1998). Deformation et rupture des versants en terrain metamorphique anisotrope apport de l'etude des ruines de sechilienne (Doctoral dissertation).

12. Zahri F. Boukelloul M, Hadji R, Talhi K (2016) Slope Stability Analysis In Open Pit Mines Of Jebel Gustar Career, Ne Algeria – A Multi-Steps Approach. Mining Science, 23: 137−146.

13. Achour, Y., Boumezbeur, A., Hadji, R. et al. (2017) Landslide susceptibility mapping using analytic hierarchy process and information value methods along a highway road section in Constantine, Algeria. Arab J.Geosci (2017) 10: 194.

14. Costet, J., Sanglerat, G., Biarez, J., & Lebelle, P. (1969). Cours pratique de mécanique des sols. Dunod.

15. Arairo W, Prunier F, Djéran-Maigre I, Darve F. A new insight into modelling the behaviour of unsaturated soils. Int. Journal for Numerical and Analytical Methods in Geo-mechanics [2013], Vol 37, p. 2629-2654

16. Mermoud A. janvier 2006, Dynamique de l'eau du sol, Ecole polytechnique Fédérale de Lausanne.

17. Rezzoug, A. Alexis, A. Kismi, M. «Influence de la marée sur la stabilité des pentes », 3èmes journées nationales de génie civil et génie côtier, Sète, 2..4 Mars 1994.

18. Pilot J. 1970. Stabilité des talus routiers. Bulletin des laboratoires routiers: Hydrauliques des sols, n° spécial, . avril 1970, 163-175,

19. Filliat G. 1981. La pratique des sols et fondations. Edition du Moniteur, p.1392:

20. Faure R.M. 1992. Méthodes de calcul de stabilité des pentes et leur validation. Journées fianco-marocaines de mécanique des sols, Paris 21-22 mai 1992, p. 17.

21. SEED, H. B., & De Alba, P. (1986). Use of SPT and CPT tests for evaluating the liquefaction resistance of sands. In Use of In Situ Tests in Geotechnical Engineering: (pp. 281-302). ASCE.

22. Bacconnet, C. Boissier D., Breul, P. «Méthodes d'évaluation du risques de liquéfaction», 23 èmes rencontres universitaires de génie civil, France, 2005.

23. Hujeux J. C « Une lois de comportement pour le chargement cyclique des sols », Revue génie parasismique, Presses de l'école nationale des ponts et chaussées, 1985.

24. Makdisi, F. I., & Seed, H. B. Simplified procedure for estimating dam and embankment earthquake-induced deformations. In ASAE Publication No. 4-77. Proceedings of the National Symposium on Soil Erosion and Sediment by Water, Chicago, Illinois, December 12-13, 1977.

25. Khansal, A. « modélisation numérique de l'essai de cisaillement rectiligne», mémoire de magister en MDS, Université de Batna, 2008.

26. Mestat Ph. «Du bon usage de l'élasticité dans les calculs de géotechnique, dans la pratique des calculs tridimensionnels en géotechnique», presses de l'école nationale des ponts et chaussées, pp 241-256, 1998.

27. Thiébot, J. Guillou, S «Calcul de stabilité des berges d'un canal», 18ème congrée français de mécanique, France, 27-31 Aout 2007.

28. Bishop A. « The use of the slip circle in the stability analysis of earth slopes», geotechnical review n°5, pp7-17, 1955.

29. Winterkorn, H. F., & Fang, H. Y. (1991). Soil technology and engineering properties of soils. In Foundation engineering handbook (pp. 88-143). Springer US.

30. Houam AK. «Amélioration de la stabilité des talus par l'utilisation des nappes horizontales de géosynthétiques», Thèse de doctorat en sciences appliquée, univ. Libre de Bruxelles, 1991.

31. Rezzoug, A., Alexis, A., & Kismi, M. (1994). Influence de la Marée sur la Stabilité des Pentes. In IIIe Journées Nationales de Génie Côtier-Génie Civil.

МАТЕМАТИЧНИЙ ПІДХІД ДО ОЦІНКИ СТАБІЛІЗУЮЧОГО ЕФЕКТУ ГЕОСИНТЕТИЧНИХ ПРОШАРКІВ ДЛЯ СТІЙКОСТІ УКОСІВ

Dahoua Lamri, 19 Місто Мохамед Бенгегуаг, Сетіф, 19000, Алжір.
https://orcid.org/0000-0002-9007-9394
Савенко Вячеслав Якович, доктор технічних наук, професор Національного транспортного університету, завідувач кафедри транспортного будівництва та управління майном
http://orcid.org/0000-0001-8174-7728
Riheb Hadji, доктор технічних наук, факультет наук про Землю, університет Сетіфа
http://orcid.org/0000-0002-9632-0812

Анотація: Зміна граничних умов є основною причиною порушення рівноваги схилів та масової трати. За нормальних кліматичних умов неконсолідовані сухі зерна залишаються стабільними для заданого внутрішнього кута тертя. Цей кут збільшується, якщо грунт трохи зволожений, оскільки поверхневий натяг між водою та частинками ґрунту має тенденцію фіксувати зерна. Під час інтенсивних опадів чи очищення від снігу інфільтрація води спричиняє зменшення значень кута тертя (φ ') та згуртованості (c') про зерна, що загрожує стійкості схилу, це останнє підкреслюється вібраціями, де відбувається зрідження ґрунту. Підтримка зниження опору міжгранульованим тертям падіння механічних характеристик ґрунту призведе до переведення кола Мора на криву розриву оболонки. Внесення геотекстильних листів може підвищити стійкість дорожніх насипів. Це здійснює стабілізуючі сили, протилежні силам, що порушують рівновагу схилу. Ці сили не враховуються методом Бішопа, який базується на великій кількості програмного забезпечення, такого як Geostudio / нахил. Наша робота полягає у розробці математичного підходу до: введення змінних значень (c ') і (φ') в критерій розриву для врахування проникнення води, введення нового параметра (F s) для врахування ефекту сейсмічні напруження, вводячи силу (r) для врахування інфільтрованої водної частини. Нарешті, в полігоні сил Єпископа беруть участь стабілізуючі сили, що створюються введенням геосинтетичних листів (Гео). Результат показує, що дія води є основною руйнівною силою схилу, а дія геотекстилю є основною стабілізуючою силою.

Ключові слова: кут внутрішнього тертя, згуртованість, геосинтетика, стійкість схилу, метод Бішопа.

Перелік посилань

1. Varnes, D.J., Int. Association of Engineering Geology Commission on Landslides, 1984.

2. Frayssines, M. (2005). Contribution à l'évaluation de l'aléa éboulement rocheux (rupture) (Doctoral dissertation, Université Joseph-Fourier-Grenoble I).

3. Antoine, P., & Giraud, A. (1995). Typologie des mouvements de versants dans un contexte opérationnel. Bulletin of Engineering Geology and the Environment, 51(1), 57-62.

4. Guadri L, Hadji R, Zahri F, Raïs K (2015). The quarries edges stability in opencast mines: A case study of the Jebel Onk phosphate mine, NE Algeria. Arabian Journal of Geosciences Arab J Geosci 8:8987–8997.

5. Hadji R, Raïs K, Gadri L, Chouabi A, Hamed Y (2017) Slope failures characteristics and slope movement susceptibility assessment using GIS in a medium scale: a case study from Ouled Driss and Machroha municipalities, Northeastern of Algeria, Arabian Journal for Science and Engineering, Arab J SciEng 42:281–300.

6. Malatrait N., 1975. Analyse et classement des mouvements gravitaires, Feuille St. Jean-de-Maurienne. Thèse d'état, Université Joseph Fourier, Grenoble I.

7. Hoek E., Brown E.T., 1980. Empirical strength criterion for rock masses. Journal of the Geotechnical engineering Division, ASCE, Vol. 106, n° GT9, 1980, 1013-1035.

8. Hoek E., 1990. Practical Rock Engineering 3-Slope Stability and Rockfalls, Chapter 9.

9. Bieniawski Z.T. Engineering Rock Mass Classifications.J. Wiley, New York, 1989.

10. Goodman, R. E., & Shi, G. H. (1985). Block theory and its application to rock engineering (p. 338). Englewood Cliffs, NJ: Prentice-Hall.

11. Vengeon, J. M. (1998). Deformation et rupture des versants en terrain metamorphique anisotrope apport de l'etude des ruines de sechilienne (Doctoral dissertation).

12. Zahri F. Boukelloul M, Hadji R, Talhi K (2016) Slope Stability Analysis In Open Pit Mines Of Jebel Gustar Career, Ne Algeria – A Multi-Steps Approach. Mining Science, 23: 137−146.

13. Achour, Y., Boumezbeur, A., Hadji, R. et al. (2017) Landslide susceptibility mapping using analytic hierarchy process and information value methods along a highway road section in Constantine, Algeria. Arab J.Geosci (2017) 10: 194.

14. Costet, J., Sanglerat, G., Biarez, J., & Lebelle, P. (1969). Cours pratique de mécanique des sols. Dunod.

15. Arairo W, Prunier F, Djéran-Maigre I, Darve F. A new insight into modelling the behaviour of unsaturated soils. Int. Journal for Numerical and Analytical Methods in Geo-mechanics [2013], Vol 37, p. 2629-2654

16. Mermoud A. janvier 2006, Dynamique de l'eau du sol, Ecole polytechnique Fédérale de Lausanne.

17. Rezzoug, A. Alexis, A. Kismi, M. «Influence de la marée sur la stabilité des pentes », 3èmes journées nationales de génie civil et génie côtier, Sète, 2..4 Mars 1994.

18. Pilot J. 1970. Stabilité des talus routiers. Bulletin des laboratoires routiers: Hydrauliques des sols, n° spécial, . avril 1970, 163-175,

19. Filliat G. 1981. La pratique des sols et fondations. Edition du Moniteur, p.1392:

20. Faure R.M. 1992. Méthodes de calcul de stabilité des pentes et leur validation. Journées fianco-marocaines de mécanique des sols, Paris 21-22 mai 1992, p. 17.

21. SEED, H. B., & De Alba, P. (1986). Use of SPT and CPT tests for evaluating the liquefaction resistance of sands. In Use of In Situ Tests in Geotechnical Engineering: (pp. 281-302). ASCE.

22. Bacconnet, C. Boissier D., Breul, P. «Méthodes d'évaluation du risques de liquéfaction», 23 èmes rencontres universitaires de génie civil, France, 2005.

23. Hujeux J. C « Une lois de comportement pour le chargement cyclique des sols », Revue génie parasismique, Presses de l'école nationale des ponts et chaussées, 1985.

24. Makdisi, F. I., & Seed, H. B. Simplified procedure for estimating dam and embankment earthquake-induced deformations. In ASAE Publication No. 4-77. Proceedings of the National Symposium on Soil Erosion and Sediment by Water, Chicago, Illinois, December 12-13, 1977.

25. Khansal, A. « modélisation numérique de l'essai de cisaillement rectiligne», mémoire de magister en MDS, Université de Batna, 2008.

26. Mestat Ph. «Du bon usage de l'élasticité dans les calculs de géotechnique, dans la pratique des calculs tridimensionnels en géotechnique», presses de l'école nationale des ponts et chaussées, pp 241-256, 1998.

27. Thiébot, J. Guillou, S «Calcul de stabilité des berges d'un canal», 18ème congrée français de mécanique, France, 27-31 Aout 2007.

28. Bishop A. « The use of the slip circle in the stability analysis of earth slopes», geotechnical review n°5, pp7-17, 1955.

29. Winterkorn, H. F., & Fang, H. Y. (1991). Soil technology and engineering properties of soils. In Foundation engineering handbook (pp. 88-143). Springer US.

30. Houam AK. «Amélioration de la stabilité des talus par l'utilisation des nappes horizontales de géosynthétiques», Thèse de doctorat en sciences appliquée, univ. Libre de Bruxelles, 1991.

31. Rezzoug, A., Alexis, A., & Kismi, M. (1994). Influence de la Marée sur la Stabilité des Pentes. In IIIe Journées Nationales de Génie Côtier-Génie Civil.